Advanced Industrial and Engineering Polymer Research xxx (xxxx) xxx

Contents lists available at ScienceDirect

KINGFA INNOVATION CHANGE LIFE

Advanced Industrial and Engineering Polymer Research

journal homepage: http://www.keaipublishing.com/aiepr

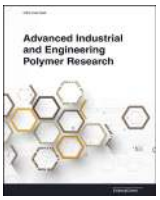

Flow visualization by Matlab® based image analysis of high-speed polymer melt extrusion film casting process for determining necking defect and quantifying surface velocity profiles

Aarati Vagga [a], Swapnil Aherrao [b], Harshawardhan Pol [b, *], Vivek Borkar [b, **]

[a] Department of Electronics & Telecommunication, Maharashtra Institute of Technology, World Peace University, Pune, India
[b] Polymer Science & Engineering Division, CSIR-National Chemical Laboratory, Pune, India

ARTICLE INFO

Article history:
Received 29 December 2020
Received in revised form
22 January 2021
Accepted 18 February 2021

Keywords:
Extrusion
Film
Necking
Velocity measurement
Image analysis
Edge detection

ABSTRACT

The primary objective of this research paper is to detect and quantify the necking defect and surface velocity profiles in high-speed polymer melt extrusion film casting (EFC) process using Matlab® based image processing techniques. Extrusion film casting is an industrially important manufacturing process and is used on an industrial scale to produce thousands of kilograms of polymer films/sheets and coated products. In this research, the necking defect in an EFC process has been studied experimentally and the effects of macromolecular architecture such as long chain branching (LCB) on the extent of necking have been determined using image processing methodology. The methodology is based on the analysis of a sequence of image frames taken with the help of a commercial CCD camera over a specific target area of the EFC process. The image sequence is then analyzed using Matlab® based image processing toolbox wherein a customized algorithm is written and executed to determine the edges of the extruded molten polymeric film to quantify the necking defect. Alongwith the necking defect, particle tracking velocimetry (PTV) technique is also used in conjunction with the Matlab® software to determine the centerline and transverse velocity profiles in the extruded molten film. It is concluded from this study that image processing techniques provide valuable insights into quantifying both the necking defect and the associated velocity profiles in the molten extruded film.

1. Introduction

High speed extrusion film casting (EFC) is an industrially important polymer processing operation used for producing thousands of kilograms of plastics films, sheetings and coated products. Typically, polyolefins make up about half of all polymers converted into films/sheets or coated products made by the EFC process. Among the polyolefins used in EFC processing, the long-chain branched low-density polyethylene (LDPE) and the mainly linear chain architecture linear low-density polyethylene (LLDPE) are widely used. The EFC process (as shown in the Fig. 1 below) consists of the following important steps: (i) polymer melt is extruded using a screw extruder from a coat hanger film/sheet die under pressure; (ii) the molten film/sheet is stretched in air for some distance (called as the take-up length or hereafter mentioned as TUL); (iii) the air-stretched film/sheet is wound using a chill-roll take-up assembly where the molten film is solidified and collected on a take-up roll. The extent of stretch that the molten film undergoes as it travels from the die exit to the chill-roll is quantified in terms of a dimensionless ratio called as the draw ratio (DR), which is defined as the ratio of the tangential velocity of the chill-roll to the linear exit velocity of the polymer melt exiting the film die [1–3]. Typical commercial EFC processes operate at very high speeds with line speeds exceeding 750 m/min.

Under steady-state and stable high-speed EFC process, two associated defects viz. necking and edge-beading are observed due to the inherent nature and the associated flow kinematics of the process. Necking is defined as the inhomogeneous reduction in the

Abbreviations: EFC, extrusion film casting; DR, draw ratio; TUL, take-up length or axial length or also called as X-span; PE, polyethylene; LDPE, low-density polyethylene; LLDPE, linear low-density polyethylene; LCB, long-chain branching; PTV, particle tracking velocimetry; CCD, charge-coupled device.

* Corresponding author.
** Corresponding author.
E-mail addresses: hv.pol@ncl.res.in (H. Pol), vv.borkar@ncl.res.in (V. Borkar).

https://doi.org/10.1016/j.aiepr.2021.02.003

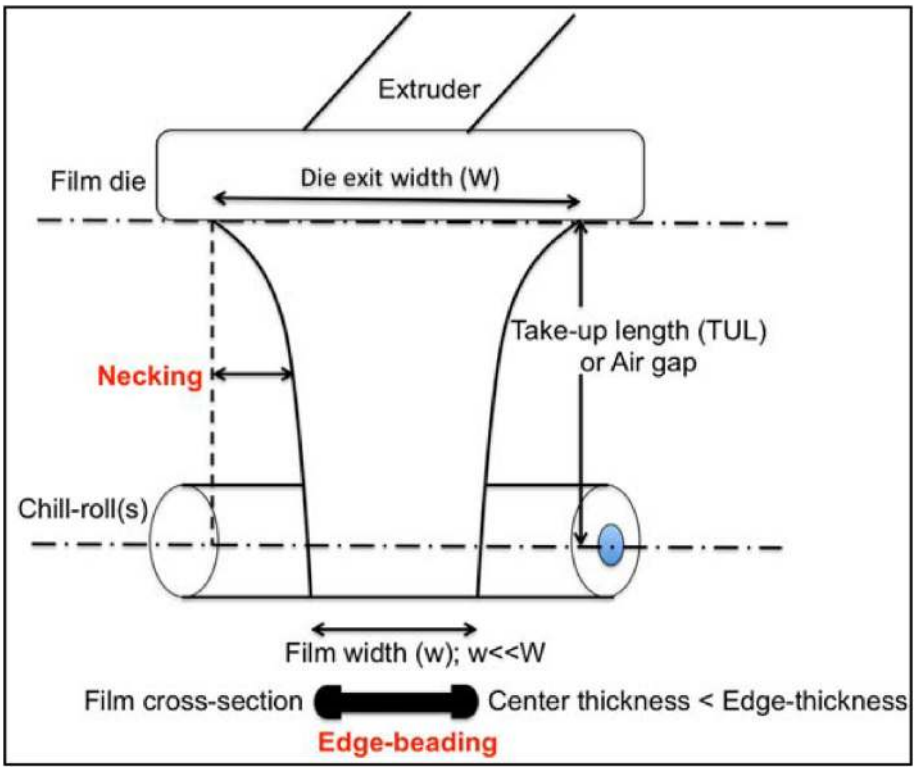

Fig. 1. Schematic of extrusion film casting process and associated defects (shown in red color).

width of the film whereas edge-beading (also called as the dog-bone defect) is defined as the inhomogeneous reduction in the thickness of the film. These two defects severly limit the production output of any commercial operation and it is desirable to significantly limit these two defects during processing. While necking reduces the useable width of the film, edge-beading leads to further width reduction since the thicker edges are usually chopped off with edge-cutters and the chopped-off edges are recycled back into the process. For e.g., if a processor starts off with melt extruding a film from a cast film die of 1 mm in width, he/she may end up with a film of only about half a meter wide at the chill-roll due to the above-mentioned defects. It is the objective of the plastics film processor to maximise his production rate and this implies that take-up speed will be increased, which usually translates to higher draw ratios (DR's). However, higher DR's mean higher extent of necking and consequently more edge-beading vis-à-vis lower DR's. In the industry, there have been significant advances in having better instrumentation & process control in producing uniformly thick films by having a feedback loop (via automated film thickness measurement) to control the die lip thickness. However, mechanisms to quantify and control necking defect are far from development. From both a scientific and a commercial viewpoint, it is imperative to study these defects thoroughly and quantify them appropriately. Indeed, due to the commercial aspect of the process, a large number of researchers have studied these defects in great detail.

In the recent past, our group at CSIR-NCL undertook a comprehensive study of the EFC process that involved a combination of detailed experiments and numerical simulations wherein we studied the effects of macromolecular chain architecture comprising of long chain branching (LCB) and molecular weight distribution (MWD) on the extent of necking during EFC for mainly polyolefins (polyethylene-PE or polypropylene-PP) having either linear and long-chain branched architectures [1–7]. The predictions from our numerical simulations were found to be in qualitative or semi-quantitative agreement with our experimental data. Our researches in this particular area have provided valuable insights into understanding the role of macromolecular architecture on polymer processing. Continuing on similar lines, our group has now begin to study & develop high-speed image processing to quantify the necking defect using image analysis techniques and whether real-time information can be fed back to processing to limit the defects. Though the realization of this objective is a little far off in the future, we are trying to take the first step in this area by analyzing the necking defect and centerline & transverse velocity profiles using off-line image analysis and we present results of this analysis in this research paper. The rest of the paper is organized as follows: we present the experimental details of the EFC process in section 2, discuss about image processing techniques in section 3, implement the system in section 4 and discuss the results in section 5 with salient conclusions presented in section 6 towards the end of the paper.

2. Experimental details

Extrusion film casting (EFC) experiments [1–3] were performed using a laboratory scale single screw extruder (ThermoHaake GmbH, Germany). A cast-film die of a coat hanger flow design and having a 100 mm fixed width and 0.3–0.6 mm adjustable thickness (or die gap) was attached to the extruder. In the present study, the die thickness was kept constant at 0.46 mm, which implied an aspect ratio (AR) of 218. A chill-roll take-up unit (having a highly-polished SS roll surface) was used for drawing and winding the extruded film. All film extrusion experiments were carried out at a constant temperature of 190 °C and at a fixed screw speed of 20 RPM, which meant a volumetric flow rate of 187 mm^3/s and a die exit velocity of 4.3 mm/s (v_0). Two distinct sets of experiments were carried out wherein the take-up length (TUL) was kept constant at

either 230 mm or at 90 mm. A simple CCD camera (Uniq Vision Inc., USA, Model: UM201) was used to video-capture the necking and the surface velocity profiles of the film during the EFC experiments [2,3]. Surface velocity profiles were determined by tracking the motion of thin paper disks (of about 2 mm diameter) that were placed on the surface of the molten film at predetermined positions along the width of the extruded film very near to the die exit. This technique is called as particle tracking velocimetry (PTV) and is shown in Fig. 2 (a & b) below. The two polymers used in this study were mainly a linear chain polyethylene (PE) such as linear low-density polyethylene (LLDPE) and a long-chain branched (LCB) polyethylene such as a low-density polyethylene (LDPE). Both polyethylene resins were donated generously by The Dow Chemical Company (USA). Since PE molten films are transparent, the CCD camera could easily capture the particle even though it was focused on the bottom surface of the molten film while the particle was placed on top surface of the molten film. The CCD camera [1–3] had a fixed shutter speed of 25 frames-per-second (fps). The shutter speed could be independently verified by capturing images of a marked disk that was located on the shaft of a calibrated stepper motor and rotated at exactly 25 RPM. Recording the rotation of the disk for 1 min created exactly 1500 images in which the particular mark at the edge of the disc achieved its original position in every 60 sequential images. This confirmed that the CCD camera was indeed acquiring images at 25 fps.

The sequence of images recorded by the CCD camera during the EFC process was analyzed using our customized Canny-based edge detection algorithm in Matlab®. The images were first corrected for camera tilt [3]. Then, a customized centroid detection algorithm was utilized to determine the positions of the particles on the surface of the film. Once the symmetry of the film was confirmed, various customized edge-detection algorithms were utilized to determine the necking profile of the film at different draw ratios. In the next section, more information about image processing techniques is given.

(a)

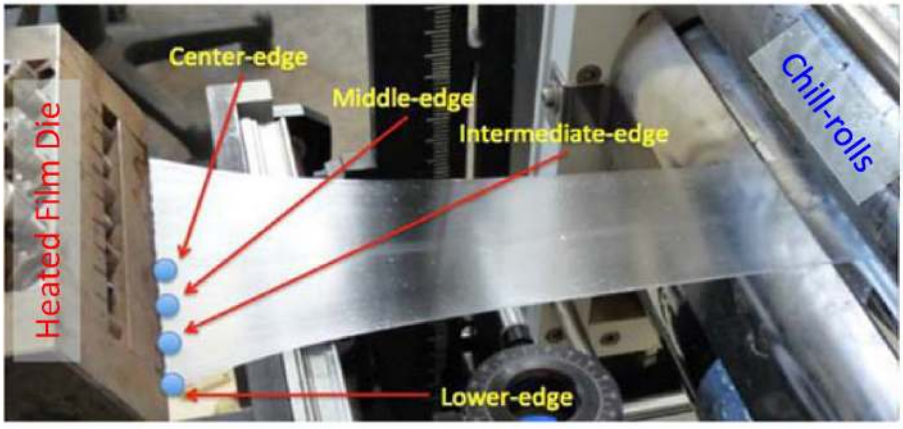

(b)

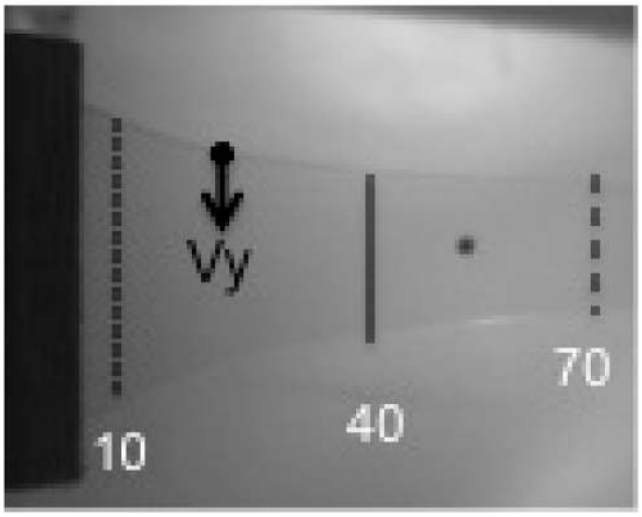

Fig. 2. PTV Measurements consisting of (a) placing thin paper disks at pre-determined positions on molten polymer film surface and (b) mapping transverse velocity profiles at various axial positions.

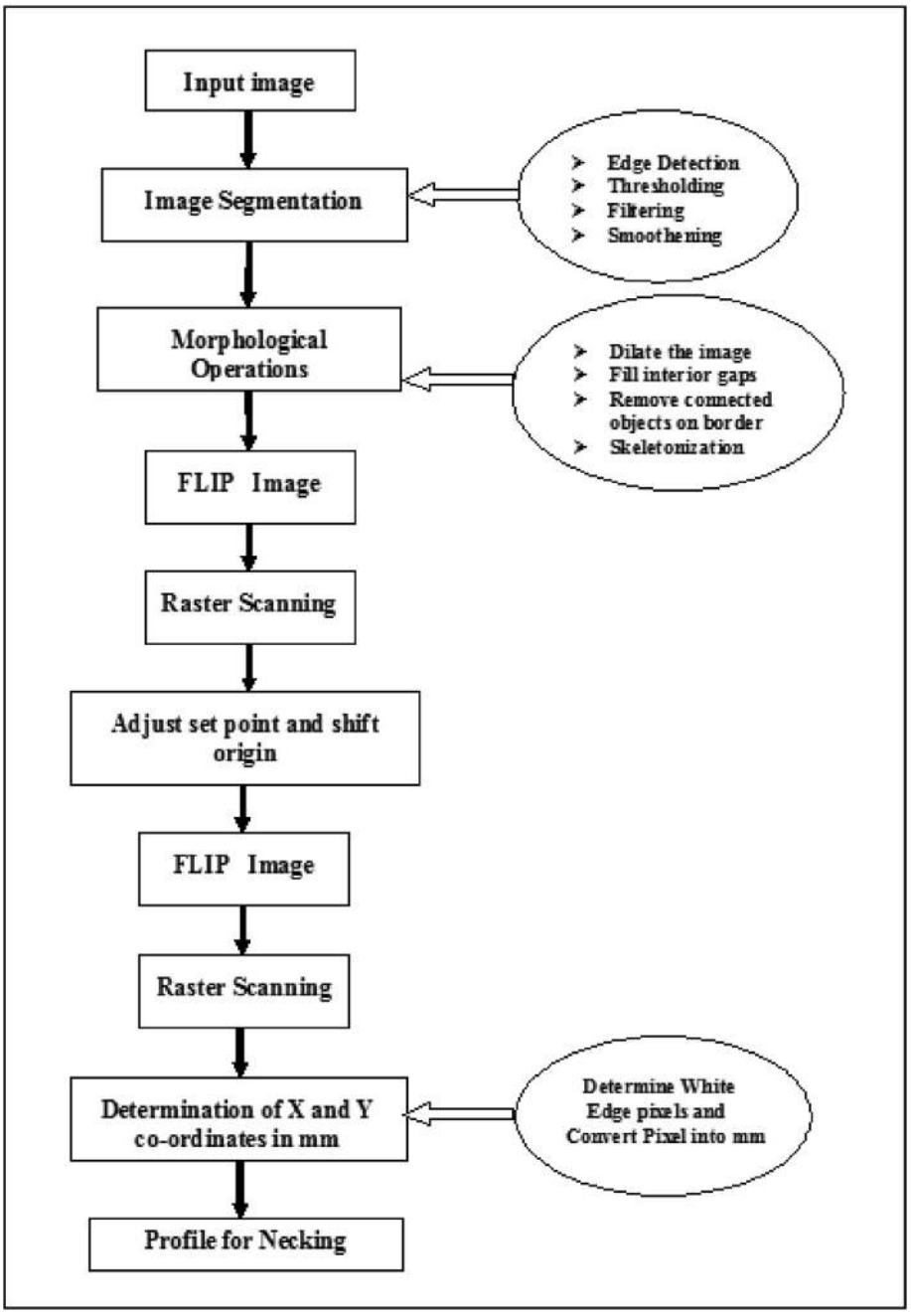

Fig. 3. Algorithm flowchart for determining necking using Matlab®.

3. Image processing techniques

3.1. Edge detection technique

Edge detection is a type of image segmentation technique, which ascertains the presence of an edge or line in an image [8,9]. Edges of an image are generally considered as a type of critical piece of information that can extracted by employing various edge detectors with accompanying methodologies [10]. The edge detection operation [11] usually starts with the inspection of the local discontinuity at each pixel element in an image [12]. The widely used edge detectors are Roberts [13], Sobel [14,15], Canny [16–18], Prewitt [19], and Krisch [20]. In EFC studies, the notable studies that have involved imaging analysis of the process to determine necking and surface velocity profiles include those by Canning & Co [21,22], Ito and coworkers [23] and our own group in the past [1–3,6].

3.2. Fundamentals of edge detection

An edge can be defined as an sudden change in brightness as one moves from one pixel to its neighbour in an image [24]. In conventional digital image processing, each image is converted into pixels. In gray-scale images, each pixel specifies the brightness level of that particular image in a designated place where zero represents black color and with 8-bit pixels, 255 represents white color. In general, the presence of an edge leads to an abrupt change in the brightness (gray scale level) of the pixels. Edge information for a

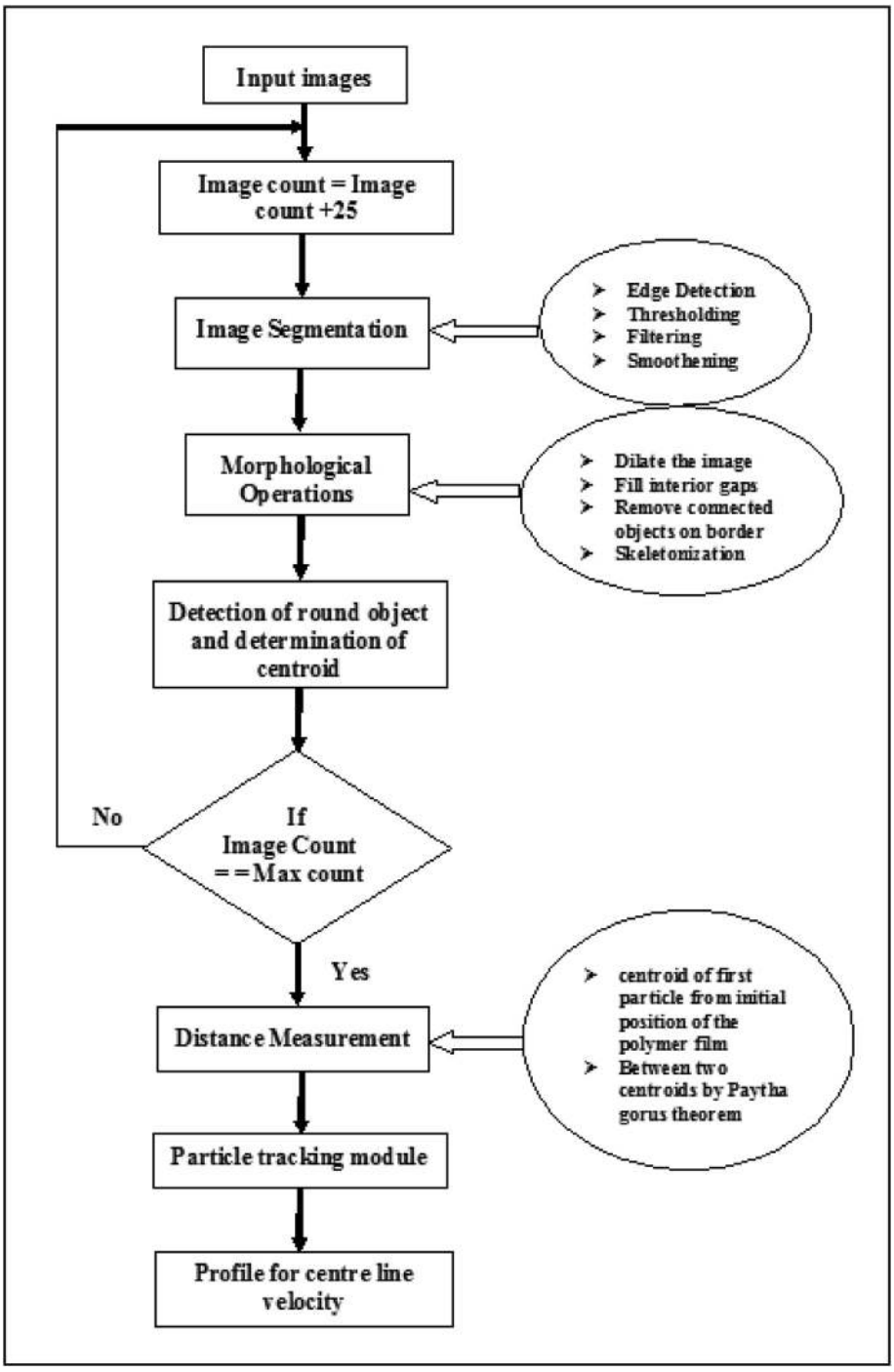

Fig. 4. Algorithm flowchart for determining velocity profiles using Matlab®.

particular pixel is typically acquired by surveying the brightness of pixels in the neighbourhood of that pixel [25]. If all of the pixels in the neighbourhood have more-or-less similar brightness, then there is usually no edge at that point. However, if some of the neighbouring pixels are much brighter than the others, then it can be theorized that there is a usually an edge at that point. Evaluating the relative brightness of pixels in a neighbourhood is mathematically equivalent to computing the derivative of the brightness. Generally, edge detection technique consists of three steps namely filtering, enhancement and detection.

3.3. Canny edge detection operator

Canny is not only one ofthe best edge detection operators but is also mathematically the most complex. Canny operator detects true edges with almost no sensitivity to noise [16–18,26]. Canny has optimized the edge detection process [26] by:

a. Maximizing the signal to noise ratio of the gradient.
b. Minimizing multiple responses to a single edge.
c. Perfect localization of the edge-by-edge localization factor.

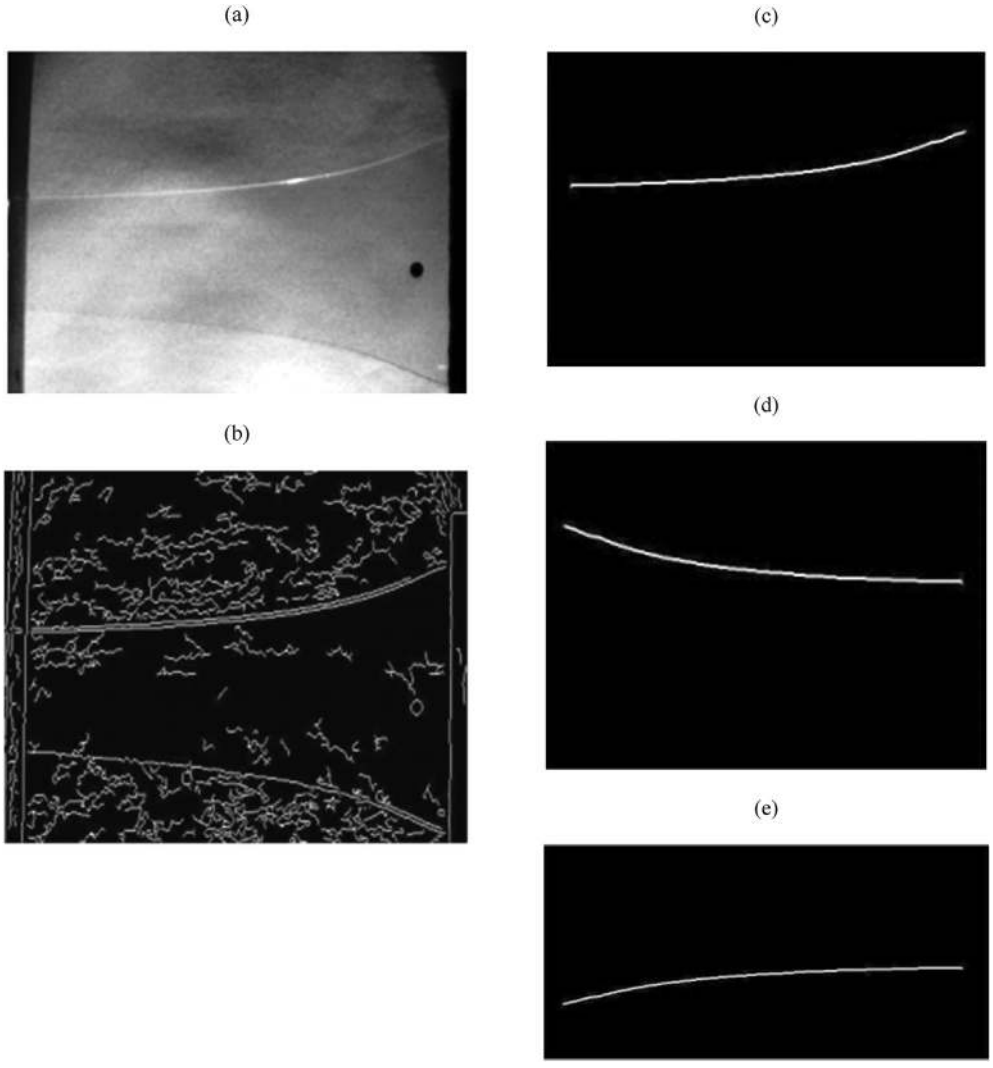

Fig. 5. (a) Original image, (b) Edge thinning I, (c) Edge after morphological operations, (d) Final Edge after Flip I, and (e) Final edge after Flip II.

3.3.1. The Canny edge detection algorithm

The Canny edge detection algorithm runs in five distinct steps [11,27,28]:

1) Smoothening: Blurring of the image to remove noise [29,30], if any.
2) Determining gradients: The edges should be marked where the gradients of the image have large magnitudes.
3) Non-maximum suppression: Only local maxima should be clearly denoted as edges.
4) Double threshold: Edges are typically determined using thresholding potential.
5) Edge tracking by hysteresis: Final edges are established by suppressing all edges that are not connected to other strong edges.

3.3.2. Operations on binary image

Morphological operations [31–33] are especially suited to the processing of binary images and greyscale images. Morphological operations [34], in general, affect the form or structure or shape of an objectand are generally applied on binary images (black & white images i.e images having only 2 colors: black & white). Morphological operations are used in either pre or post processing

Table 1
Representative values for necking profile for LDPE film at a DR = 17 for a TUL of 230 mm.

Dist. along centerline of film (mm)	Film half width (mm)
0	50.45454545
10	45.90909091
20	40.90909091
30	37.72727273
40	34.54545455
50	31.81818182
60	29.09090909
70	27.27272727
80	25.45454545
90	23.63636364
100	22.27272727
110	22.27272727
120	19.54545455
130	18.18181818
140	16.81818182
160	15.45454545
170	15
180	14.54545455
190	14.09090909
200	12.72727273
210	12.27272727
212	12.27272727

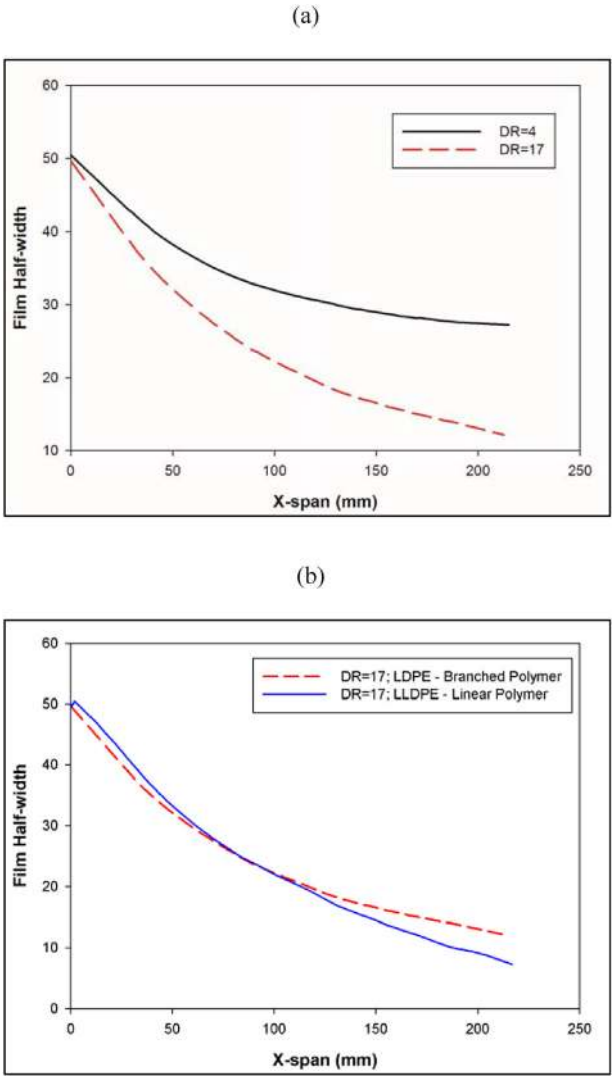

Fig. 6. Necking profile determined using Matlab for (a) LDPE film at two distinct DR's of 4 and 17 and (b) comparision between the two separate polymers LDPE and LLDPE at an equivalent DR of 17 and for a TUL of 230 mm.

(filtering, thinning &/or trimming) of images or for obtaining a representation or depiction of the shape of objects or regions such as boundaries or skeletons [35,36].

4. System implementation

4.1. System algorithm for detecting edges and determining the necking profile

The system was implemented in image processing using Matlab®. Image segmentation was obtained by following sequence:

a) Canny-based customized edge detection method
b) Thresholding
c) Filtering
d) Smoothening

Clear edges could be obtained by using a customized Canny-based edge detection algorithm on an image (captured by CCD camera) of necking of a polymer film during EFC process.

Various morphological operations were then used such as:

a) Dilating the image
b) Filling the interior gaps
c) Removing the connected objects on the image border
d) Skeletonization

Finally, by scanning of a clear edge obtained after the morphological operations, *x* and *y* coordinates were successfully obtained for determination and evaluation of necking phenomenon.

Figure 3 below displays our algorithm flowchart for determining the necking phenomenon in an EFC process using Matlab®.

4.2. System algorithm for particle detection and determination of surface velocity profiles

Particle detection and tracking was done by using customized algorithms and various morphological operations using Matlab®. The velocity of film was determined by finding centroid of particle and tracking of particle on the surface of the moving molten polymeric film. For particle detection, detection of the round object and determination of centroid of particle was necessary. Various distance measurement could be done such as centroid of first particle from initial position of the polymer film and between two centroids by using the widely recognized Pythagoras theorem. Finally, by particle tracking algorithms, the profile for centre line velocity could be determined. In a similar manner, transverse velocity profiles could also be determined by mapping the *x* and *y* coordinates of particles kept at the different positions along the width of the molten polymer film surface as these particles traveled from the die exit towards the chill-roll. Fig. 4 displays the algorithm flowchart for determining the surface velocity profiles along the axial and transverse directions of a molten extruded polymer cast film.

5. Results and discussions

5.1. Edges by Canny and morphological operations

The data set used in this work has large dimensions and to reduce the computational complexity and time, it is desirable to reduce the dimensions of the data. Large size high-quality images are therefore cropped with proper dimensions. For detecting clear edges, the Canny algorithm with various morphological operations are used. Edges by Canny and the associated morphological operations are shown in Fig. 5 (a) through (e).

Figure 5(a) displays one image from a sequence of images captured for say a LDPE film extrusion at a fixed draw ratio (DR) and take-up length (TUL). After applying the requisite morphological operations on this particular image and our customized Canny-based edge detection algorithm, a single clear edge can be detected successfully. It is enough to apply this methodology on any image in a sequence since the images are very similar to each other as the process is at steady-state. In other words, in steady-state and at a fixed DR and TUL, dimensional changes in the molten extruded polymer film do not take place with respect to time. A profile of necking can then be constructed using *x* coordinates as the axial length along the take up length or TUL (or also called as X-span) in mm and *y* coordinates as film half-width in mm (as shown in Table 1) for DR of 4 and 17. The necking profile for the two different polymers determined using our customized algorithm in Matlab®software are shown in Fig. 6 (a) & (b) below.

A user-friendly GUI using Matlab®software was also developed by our team in our laboratory for the purpose of allowing students/staff to determine necking and surface velocity profiles by inputting the relevant imaging data into Matlab®. This allowed the students/staff who were not competent in using Matlab® software to

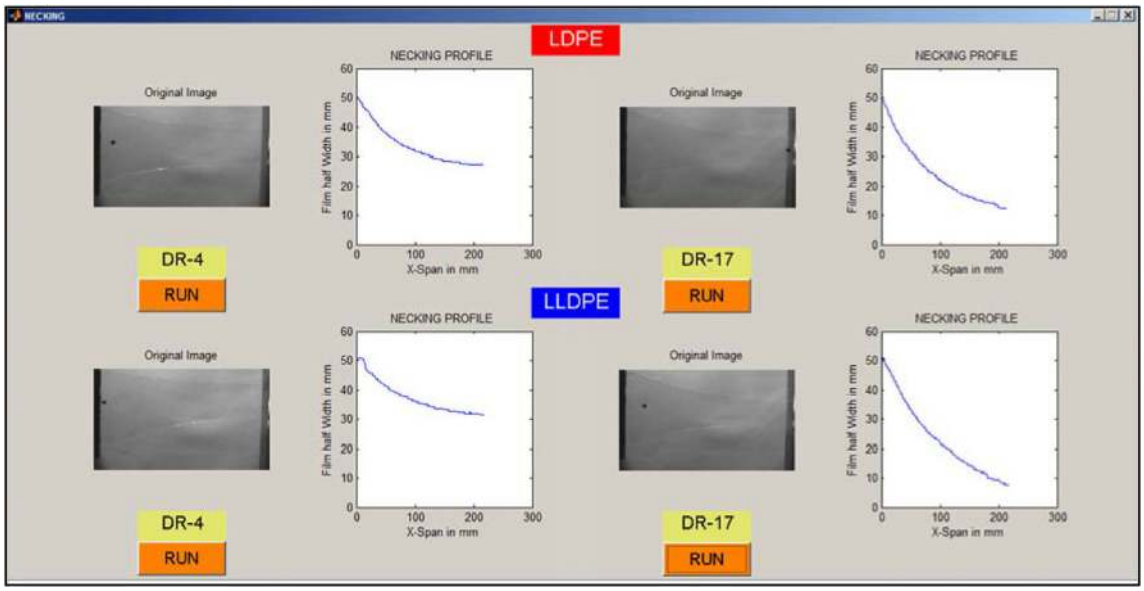

Fig. 7. User-friendly GUI developed using Matlab® software for determining necking and surface velocity profiles.

determine the necking and surface velocity profiles independently. A screen-shot of this user-friendly GUI, displaying the necking profiles of various extruded films under study, is shown in Fig. 7 below. The steps involved in creating this user-friendly GUI consisted of:

1. Based on user feedback, a GUI layout was first conceptualized using pen and paper.
2. From Matlab®software, using the "Guide" radio button, under the "Create New GUI", we selected a "Blank GUI (default)".
3. In the created blank *.fig file, various elements of the conceptualized GUI were inserted including various graphs (consisting of axes boxes, title, scale, etc.), texts, and radio push buttons.
4. This *.fig file was saved which created a *.m file in which various functions for the above-mentioned elements were created.
5. For each created radio push button function (for e.g. RUN in our GUI figure listed below) in the *.m file, a unique Matlab®code was executed for that particular condition (say DR = 17 for a LDPE polymer film) giving its output (say the necking profile) in the associated "axes" box.

In this manner, a user could obtain necking (or surface velocity profiles) from Matlab® software based image analysis.

It is clear from the necking profiles (Fig. 6 (a) above) determined using our modified algorithm procedure in Matlab® that necking increases with increase in draw ratio at a constant TUL; higher the draw ratio, higher is the necking and this is generally true for any polymeric film. The necking profile for the lower DR of 4 is always situated higher than that for the higher DR of 17. When necking profiles between the two polyethylenes at an equivalent DR and TUL is compared, it is observed that the necking for the long-chain branched LDPE polymer is always lower than that as compared to the mainly linear chain polymer LLDPE. There are some interesting features observed from the necking profile for the two different polymers shown in Fig. 6(b). It is observed that the mainly linear chain polymer LLDPE film displays a prominent extrudate swell and also a higher resistance to necking just near the die exit as compared to the long-chain branched LDPE film. As the film progresses further towards the chill-roll, at a certain point along the axial length, the profiles reverse and the linear LLDPE film displays a higher necking vis-à-vis the branched LDPE film. Table 1 below displays representative values of the necking profile for the branched LDPE film at a constant DR of 17 and a constant TUL of 230 mm.

As mentioned before, due to a pre-dominant viscoelastically driven extrudate swell just near the die exit, the film half-width is slightly higher than the half-width of the die (50 mm). Due to the necking defect, the film half-width then rapidly keeps on decreasing as the film travels towards the chill-roll. Successful detection of necking of extruded molten polymer films is a very important finding in this area of research and utilization of such image processing techniques enables researchers/plastics film processors to quickly quantify the defects and take remedial actions. The important conclusions that could be drawn from undertaking the Matlab® based edge detection study include the following important findings: (i) presence of long-chain branching (LCB) reduces necking of films; (ii) film necking increases with increase in DR at a fixed TUL; and (iii) film necking increases with increase in TUL at a fixed DR.

5.2. Centreline velocity profiles

Centreline velocity profiles for representative DRs of 4 and 17 for the LCB containing LDPE film with respect to X-span are shown in Fig. 8(a) below. Table 2 gives representative values of centerline velocity data at a DR of 4 for the mainly linear chain LLDPE film. In general, the surface velocity is found to increase along the axial direction. As shown in Fig. 8(b), the centerline velocity profile is mostly exponential increase for linear chain polymers such as LLDPE while it tends to become more-or-less linear increase for long-chain branched polymers such as LDPE. The centerline velocity values for the branched LDPE are always higher than those for the linear chain LLDPE at equivalent X-span locations; the reasoning behind this occurrence is based on differences in the viscoelasticity between the two materials at equivalent processing temperature, DR and TUL [1,2]. In other words, the centerline velocity profile for the branched LDPE polymer film is always situated higher than that for the mainly linear chain LLDPE polymer film throughout the TUL at equivalent DRs. It is also interesting to note that the linear chain LLDPE polymer film, which shows a

(a)

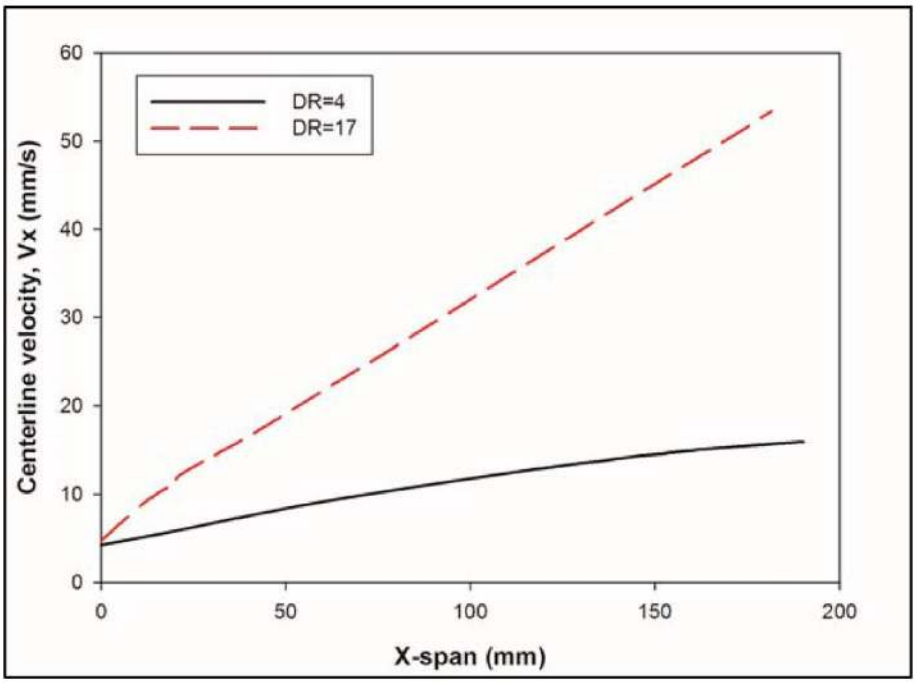

(b)

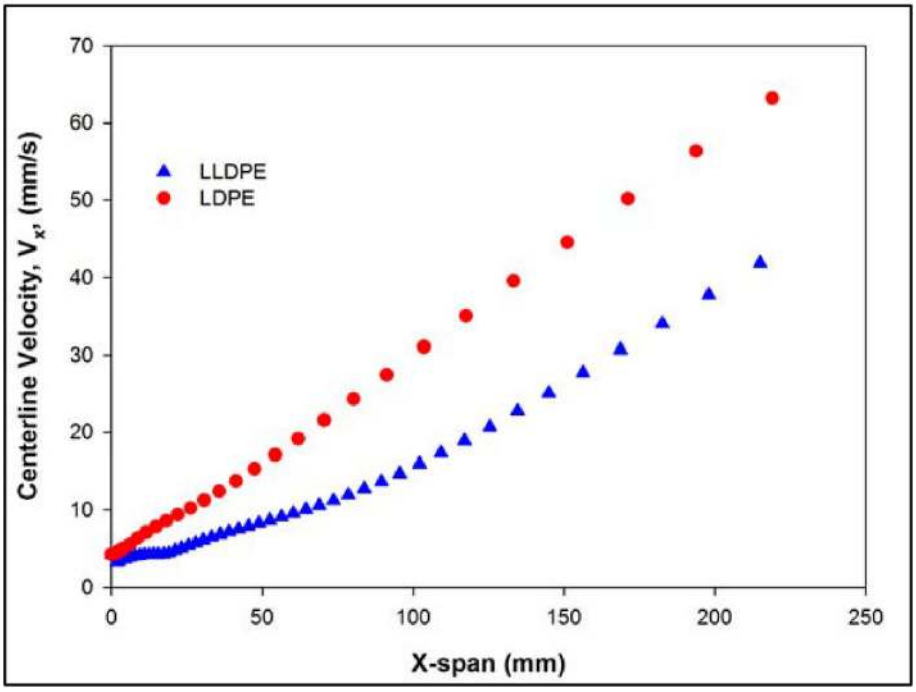

Fig. 8. Matlab detected Centerline velocity profile for (a) LDPE film at two distinct DR's and at a constant TUL of 230 mm and (b) comparision between LDPE and LLDPE film at a constant DR of 17 and TUL of 230 mm.

Table 2
Representative values for centerline velocity for a DR = 4 for LLDPE Film for a TUL of 230 mm.

Dist. along centerline of film (mm)	Centerline velocity, V_x in (mm/s)
0	4.205177315
4.567003793	4.569959979
9.475532219	4.91035811
14.93652365	5.463198555
20.83216111	5.901605532
27.17362609	6.341575762
34.255095	7.084479608
41.98289788	7.732869575
50.52072889	8.539090662
59.67502554	9.1581571
69.61080007	9.937534407
80.11386662	10.50377639
91.32034373	11.20735291
103.357775	12.0385337
116.0096924	12.65355454
129.6527602	13.64386508
144.0950203	14.44750236
158.9353315	14.84386026
174.3985547	15.47180714
190.2775144	15.88112266
174.3985547	15.47180714
190.2775144	15.88112266

viscoelastically driven extrudate swell near the die exit also shows a small region of lower velocities just near the die exit where the films actually slows down due to the swell and then it speed ens up as the effect of swell disappears at higher axial locations.

5.3. Transverse velocity profiles

In the earlier section of this paper, data for centerline surface velocity (V_x) profiles obtained from tracer particle-tracking velocimetry (PTV) technique was presented. As mentioned before in the experimental section, tracer particles were also placed on the surface of the extruded film at other positions along the film width (apart from centerline position). These positions were denoted as lower edge, intermediate edge, and middle edge. Tracking the motion of these particles allowed for the measurement of the transverse velocity (V_y) profiles at various *axial* locations on the film and also at various transverse locations as well.

Figure 9 (a) displays the transverse velocity as a function of *axial* location for the branched LDPE 170A at a TUL of 90 mm for a low DR of 4 and a high DR of 17. It is readily observed that the transverse velocities at the three different positions (lower edge, intermediate edge and middle edge) steadily decrease as a function of *axial* location. Maximum V_y occurs just at the exit of the die where the extruded film comes out and immediately starts necking. The V_y values at the centerline are zero as expected. For both PE's, as the DR increases, the V_y values at the outermost edge (labeled lower edge) increase as the film experiences enhanced necking.

Figure 9 (b) displays the transverse velocity (V_y) profiles as a function of the width (Y) direction at different *axial* locations for the LCB containing LDPE resin at a high DR of 17. The transverse velocity profiles for both polyethylene films are found to be nearly linear, which is one of the principal flow kinematics assumptions while modeling the EFC process [1–3]. Thus, comparisons between our CFD or numerical predictions (from our earlier research papers and shown in references listed above) and experimental data are justified. It is clear from Fig. 9 (b) above that as one moves down the centerline of the film (*axial* locations), the *Vy* values decrease at any given Y-location.

Transverse velocity profiles are crucial in determining the extent of necking that a polymer film will undergo for a particular DR and

(a)

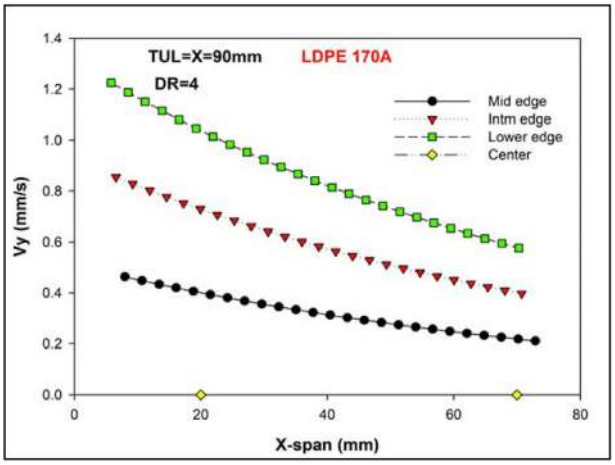

(b)

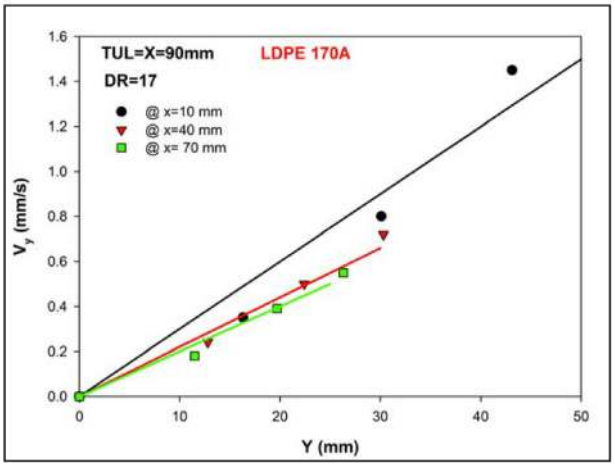

Fig. 9. Transverse velocity profiles for LDPE film at a constant TUL of 90 mm along (a) the axial direction at a DR = 4 and along (b) the transverse direction at DR = 17.

TUL combination. At this point, it is felt that additional detailed PTV experiments are required to obtain transverse velocity profiles with even better accuracy and resolution so that they can be directly compared with 2-D FEM numerical simulations of the EFC process that are planned in the future.

6. Conclusions

Experimental extrusion film casting (EFC) studies were performed on commercial polyethylene resins of mainly linear chain and long-chain branched macromolecular architectures. The current research shows that it is possible to determine the necking phenomena from edge detection and surface velocity profiles from particle tracking using custom modified algorithms in Matlab®. In this research a customized Canny based edge-detection algorithm was used along with various morphological operations. This algorithm enabled determination of necking profiles of molten polymer film edges in the extrusion film casting process. Centreline (or axial) and transverse surface velocity profiles could be determined successfully using Matlab® based customized centroid detection and tracking algorithms. In general, it was determined from image

processing studies using Matlab® that both the commercial polyethylene films displayed necking as the draw ratio increased with the branched LDPE film displaying a higher resistance towards necking as compared to the mainly linear chain LLDPE film. Interesting features such as extrudate swell just near the die exit could be determined successfully. From the surface velocity profiles, it was found that the branched LDPE film displayed a nearly linearly increasing centerline velocity profile while the mainly linear chain LLDPE film displayed an exponentially increasing centerline velocity profile. For both polyethylene films, as the DR increased, the transverse velocity values at the outermost edge (labeled lower edge) increase as the film experienced enhanced necking. Additionally, it was found from image processing that the transverse velocity profiles along the axial direction for both polyethylene films were found to be nearly linear. In conclusion, image processing using customized Matlab® based algorithms have been successful to a great extent in determining necking and surface velocity profiles in polymer melt extrusion film casting process. Future work in this area will involve developing a robust Matlab® based imaging system that will quantify the necking profile, surface velocity patterns and thickness profiles in real time and feed the data back to process control system to make necessary changes to the process to limit these unwanted defects and enhance productivity of the extrusion film casting process.

Conflict of interest

On behalf of all authors, the corresponding author states that there is no conflict of interest.

Acknowledgements

The authors (SRA, HVP and VVB) would also like to acknowledge their parent organization, CSIR-National Chemical Laboratory (CSIR-NCL) for giving them the necessary support to pursue this exciting field of study. We also thank Dr. Teresa Karjala of The Dow Chemical Company for donating the polyethylene materials used in this study.

References

[1] H.V. Pol, S.S. Thete, P. Doshi, A.K. Lele, Necking in extrusion film casting: the role of macromolecular architecture, J. Rheol. 57 (2013) 559–583, https://doi.org/10.1122/1.4788911.
[2] H. Pol, S. Banik, L.B. Azad, S. Thete, P. Doshi, A. Lele, Nonisothermal analysis of extrusion film casting process using molecular constitutive equations, Rheol. Acta 53 (2014) 85–101, https://doi.org/10.1007/s00397-013-0739-x.
[3] K. Chikhalikar, S. Banik, L.B. Azad, K. Jadhav, S. Mahajan, Z. Ahmad, et al., Extrusion film casting of long chain branched polypropylene, Polym. Eng. Sci. 55 (2015) 1977–1987, https://doi.org/10.1002/pen.24039.
[4] H.V. Pol, S.S. Thete, Necking in extrusion film casting: numerical predictions of the maxwell model and comparison with experiments, J. Macromol. Sci. Part B: Phys. 55 (2016) 984–1006, https://doi.org/10.1080/00222348.2016.1225556.
[5] R. Dhadwal, S. Banik, P. Doshi, H. Pol, Effect of viscoelastic relaxation modes on stability of extrusion film casting process modeled using multi-mode Phan-Thien-Tanner constitutive equation, Appl. Math. Model. 47 (2017) 487–500, https://doi.org/10.1016/j.apm.2017.03.010.
[6] S.S. Thete, P. Doshi, H.V. Pol, New insights into the use of multi-mode phenomenological constitutive equations to model extrusion film casting process, J. Plastic Film Sheeting 33 (2017) 35–71, https://doi.org/10.1177/8756087915627843.
[7] S. Chougale, D. Rokade, T. Bhattacharjee, H. Pol, R. Dhadwal, Non-isothermal analysis of extrusion film casting using multi-mode Phan-Thien Tanner constitutive equation and comparison with experiments, Rheol. Acta 57 (2018) 493–503, https://doi.org/10.1007/s00397-018-1095-7.
[8] O.P. Verma, R. Sharma, Newtonian gravitational edge detection using gravitational search algorithm, in: 2012 Int. Conf. Commun. Syst. Netw. Technol., IEEE, 2012, pp. 184–188, https://doi.org/10.1109/CSNT.2012.48.
[9] M. Agarwal, V. Singh, A methodological survey and proposed algorithm on image segmentation using genetic algorithm, Int. J. Comput. Appl. 67 (2013) 7–17.
[10] D. Yadav Madhulika, P. Gupta Madhurima, J. Singh G Kaur, et al., Implementing edge detection for medical diagnosis of a bone in Matlab, in: 2013 5th Int. Conf. Comput. Intell. Commun. Networks, IEEE, 2013, pp. 270–274, https://doi.org/10.1109/CICN.2013.64.
[11] Gaurav Mandloi, A survey on feature extraction techniques for color images, Int. J. Comput. Sci. Inf. Technol. 3 (2013) 14–18.
[12] S. Bamba, R. Mahajan, Performance evaluation of modified color based edge detection of remote sensing images using fuzzy logic, Int. J. Adv. Res. Comput. Sci. Software Eng. 4 (2014) 334–343.
[13] L.G. Roberts, Machine Perception of Three-Dimensional Soups, Massachusetts Institute of Technology, 1963.
[14] Chunxi Ma, Wenshuo Gao, Lei Yang, Zhonghui Liu, An improved Sobel algorithm based on median filter, in: 2010 2nd Int. Conf. Mech. Electron. Eng., IEEE, 2010, pp. V1-88–V1-92, https://doi.org/10.1109/ICMEE.2010.5558590.
[15] Wenshuo Gao, Xiaoguang Zhang, Lei Yang, Huizhong Liu, An improved Sobel edge detection, in: 2010 3rd Int. Conf. Comput. Sci. Inf. Technol., IEEE, 2010, pp. 67–71, https://doi.org/10.1109/ICCSIT.2010.5563693.
[16] J. Canny, A computational approach to edge detection, IEEE Trans. Pattern Anal. Mach. Intell. PAMI-8 (1986) 679–698, https://doi.org/10.1109/TPAMI.1986.4767851.
[17] M. Ali, D. Clausi, Using the Canny edge detector for feature extraction and enhancement of remote sensing images, in: IGARSS 2001. Scanning Present Resolv. Futur. Proceedings. IEEE 2001 Int. Geosci. Remote Sens. Symp. (Cat. No.01CH37217), IEEE, 2001, pp. 2298–2300, https://doi.org/10.1109/IGARSS.2001.977981.
[18] C.-Z. Yanlong-Chen, Improved edge detection algorithm based on Canny operator, Comput. Appl. Softw. 25 (2008) 51–53.
[19] A. Seif, Mohammad Mohammadpour Salut, M.N. Marsono, A hardware architecture of Prewitt edge detection, in: 2010 IEEE Conf. Sustain. Util. Dev. Eng. Technol., IEEE, 2010, pp. 99–101, https://doi.org/10.1109/STUDENT.2010.5686999.
[20] M. Sharifi, M. Fathy, M.T. Mahmoudi, A classified and comparative study of edge detection algorithms, in: Proceedings. Int. Conf. Inf. Technol. Coding Comput., IEEE Comput. Soc, 2002, pp. 117–120, https://doi.org/10.1109/ITCC.2002.1000371.
[21] K. Canning, A. Co, Edge effects in film casting of molten polymers, J. Plastic Film Sheeting 16 (2000) 188–203, https://doi.org/10.1106/G0MF-N3HC-3DJ1-WLJ1.
[22] K. Canning, B. Bian, A. Co, Film casting of a low density polyethylene melt, J. Reinforc. Plast. Compos. 20 (2001) 366–376, https://doi.org/10.1106/RBAG-6RCL-577G-HWDD.
[23] H. Ito, M. Doi, T. Isaki, M. Takeo, K. Yagi, 2D flow analysis of film casting process, J. Soc. Rheol. Japan. 31 (2003) 149–155.
[24] A. Prabhakar, Edge Detection Theory. http://edge.kitiyo.com/tags/roberts, 2014.
[25] UK Essays, Edge Detection in Blurred Images Biology Essay, UK Essays, 2015. https://www.ukessays.com/essays/biology/edge-detection-in-blurred-images-biology-essay.php?cref=1.
[26] Z.E.M. Osman, F.A. Hussin, N.B.Z. Ali, Optimization of processor architecture for image edge detection filter, in: 2010 12th Int. Conf. Comput. Model. Simul., IEEE, 2010, pp. 648–652, https://doi.org/10.1109/UKSIM.2010.123.
[27] Y. Chaudhari, T. Dave, S. Barade, S. Mane, S. Sangwe, A. Devare, 3 - layer security using face recognition in cloud, Int. J. Comput. Sci. Netw. 1 (2012) 2–6.
[28] P. Nithya, C. Thirumarai Selvi, R. Sushakar, An efficient edge detection algorithm based on fuzzylogic for image processing and synthesize in Xilinx, Int. J. Adv. Res. Trends Eng. Technol. 2 (2015) 182–188.
[29] S.R. Joshi, R. Koju, Study and comparison of edge detection algorithms, in: 2012 Third Asian Himalayas Int. Conf. Internet, IEEE, 2012, pp. 1–5, https://doi.org/10.1109/AHICI.2012.6408439.
[30] P.P. Gangal, V.R. Satpute, K.D. Kulat, A.G. Keskar, Application of image processing for spray angle measurement of furnace oil gun nozzle, in: 2012 2nd Int. Conf. Power, Control Embed. Syst., IEEE, 2012, pp. 1–5, https://doi.org/10.1109/ICPCES.2012.6508043.
[31] T. Chen, Q.H. Wu, R. Rahmani-Torkaman, J. Hughes, A pseudo top-hat mathematical morphological approach to edge detection in dark regions, Pattern Recogn. 35 (2002) 199–210, https://doi.org/10.1016/S0031-3203(01)00024-3.
[32] J.-F. Rivest, Morphological operators on complex signals, Signal Process. 84 (2004) 133–139, https://doi.org/10.1016/j.sigpro.2003.10.002.
[33] C. NagaRaju, S. NagaMani, G. RakeshPrasad, S. Sunitha, Morphological edge detection algorithm based on multi-structure elements of different directions, Int. J. Inf. Commun. Technol. Res. 1 (2011) 37–43.
[34] G. Mani, P.V. Gounder, An efficient high resolution medical image segmentation technique using holder exponent, J. Appl. Sci. 12 (2012) 2332–2337, https://doi.org/10.3923/jas.2012.2332.2337.
[35] M.A. Ahmed, H.M. Ebied, A.M. Salem, M.P. Image, V. Database, Palm vein preprocessing image based on, Int. J. Emerg. Trends Technol. Comput. Sci. 3 (2014) 200–204.
[36] D. Joshi, S. Pansare, Combination of multiple image features along with KNN classifier for classification of Marathi barakhadi, in: 2015 Int. Conf. Comput. Commun. Control Autom., IEEE, 2015, pp. 607–610, https://doi.org/10.1109/ICCUBEA.2015.124.